Environ Monit Assess (2025) 197:653
https://doi.org/10.1007/s10661-025-14098-z

RESEARCH

Long-term monitoring of particulate matter in an Asian community using research-grade low-cost sensors

Tzu-Chi Chieh · Shih-Chun Candice Lung · Li-Te Chang · Chun-Hu Liu · Ming-Chien Mark Tsou · Tzu-Yao Julia Wen

Received: 15 November 2024 / Accepted: 29 April 2025

Abstract Particulate matter with an aerodynamic diameter of 2.5 µm or less ($PM_{2.5}$) poses significant health risks, necessitating comprehensive exposure assessment. Long-term community monitoring can provide representative exposure levels for environmental epidemiological studies. This study deployed nine research-grade low-cost sensors (AS-LUNG-O) for 3.5 years of street-level $PM_{2.5}$ monitoring in an Asian community, evaluating temporospatial variations, hotspots, and emission sources. The hourly mean $PM_{2.5}$ concentrations from December 2017 to July 2021 were 24.3 ± 14.1 µg/m^3. $PM_{2.5}$ levels were typically higher in winter, on weekends, and during religious events compared to summer, weekdays, and typical days, with some peak concentrations occurring randomly. Daytime $PM_{2.5}$ levels generally exceeded nighttime background levels by 30–50%, with certain religious activities causing up to 80% increases. Spatial analysis identified temples and markets as pollution hotspots. Using a generalized additive mixed model, we found that the COVID-19 pandemic shutdown and higher wind speeds negatively impacted PM concentrations. Religious events, traffic, and vendors were significant PM sources, continually influencing community air quality throughout the 3.5-year monitoring period. This study demonstrates the value of long-term PM monitoring in capturing unexpected peaks, identifying critical sources, and revealing intricate temporospatial distributions. Research-grade low-cost sensor networks complement traditional monitoring stations by

Supplementary Information The online version contains supplementary material available at https://doi.org/10.1007/s10661-025-14098-z.

T.-C. Chieh · S.-C. C. Lung (✉) · C.-H. Liu · M.-C. M. Tsou · T.-Y. J. Wen
Research Center for Environmental Changes, Academia Sinica, No. 128, Sec. 2, Academia Rd., Nangang Dist., Taipei 115, Taiwan
e-mail: sclung@rcec.sinica.edu.tw

T.-C. Chieh
e-mail: tcchieh@gate.sinica.edu.tw

C.-H. Liu
e-mail: lch0909@gate.sinica.edu.tw

M.-C. M. Tsou
e-mail: marktsou09@gate.sinica.edu.tw

T.-Y. J. Wen
e-mail: zywen@gate.sinica.edu.tw

S.-C. C. Lung
Department of Atmospheric Sciences, National Taiwan University, No. 1, Sec. 4, Roosevelt Rd., Daan Dist., Taipei 106, Taiwan

S.-C. C. Lung
Institute of Environmental and Occupational Health Sciences, National Taiwan University, No. 17, Xuzhou Rd., Zhongzheng Dist., Taipei 100, Taiwan

L.-T. Chang
Department of Environmental Engineering and Science, Feng Chia University, No. 100, Wenhua Rd., Xitun Dist., Taichung 407, Taiwan
e-mail: ltechang@fcu.edu.tw

Published online: 14 May 2025

facilitating source identification in targeted communities and providing representative PM exposure data for long-term environmental epidemiological research.

Keywords PM microsensor · PM source evaluation · Neighborhood air quality · Asian culture sources · GIS mapping of PM

Introduction

Both short-term and long-term exposure to particulate matter (PM) has been consistently linked to adverse health effects (Alexeeff et al., 2021; Brunekreef & Holgate, 2002; Kioumourtzoglou et al., 2016; WHO, 2021, 2023), with $PM_{2.5}$ (particulate matter with an aerodynamic diameter ≤2.5 μm) posing particularly significant risks. Growing public health concerns have intensified demands for effective $PM_{2.5}$ source control strategies to reduce exposure and associated health risks. While industrial emissions have traditionally been the primary regulatory focus, increasing attention now centers on community-level emission sources that may disproportionately contribute to residents' daily exposure levels (Farooqui et al., 2023; Heintzelman et al., 2023; Rose Eilenberg et al., 2020).

$PM_{2.5}$ exposure intensity and contributing sources within communities exhibit significant regional variations, shaped by distinct cultural practices and lifestyle factors across different countries (Karagulian et al., 2015). Taiwan exemplifies this phenomenon with its numerous culture-specific $PM_{2.5}$ emission sources, including food frying and incense burning for religious worship, which are substantially less common in Western societies (Lung et al., 2007, 2014, 2020a; Wu et al., 2017). Furthermore, Taiwan's distinctive urban characteristics—high population density coupled with mixed residential-commercial zoning—create environments where residential communities face concentrated traffic-related emissions (Lee et al., 2023; Lung et al., 2014). These unique conditions underscore the importance of community-level $PM_{2.5}$ monitoring to accurately assess residents' actual exposure patterns. A network with multiple sensors deployed along the community streets offers a promising approach to identify and characterize the diverse $PM_{2.5}$ sources that residents encounter in their daily activities.

The emergence of low-cost sensors (LCSs) has revolutionized community-level air quality monitoring (Gao et al., 2015; Jiao et al., 2016; Lewis et al., 2018), especially as researchers have successfully addressed initial challenges in sensor stability and calibration through innovative methodological approaches (Bai et al., 2020; Bulot et al., 2019; Chu et al., 2020; Feenstra et al., 2019; Feng et al., 2024; Jayaratne et al., 2020; Kelly et al., 2017; Lee et al., 2024; Wang et al., 2020a). LCSs are capable of collecting high-resolution observations in both temporal and spatial scales, making them suitable for stable and widespread application in community monitoring. They have been increasingly installed to monitor $PM_{2.5}$ levels within communities worldwide (Connolly et al., 2022; Hsu et al., 2020; Jiao et al., 2016; Johnson et al., 2018; Lung et al., 2020a; Rojas González & Montilla-Rosero, 2025). Deploying LCS networks for community $PM_{2.5}$ monitoring is particularly valuable across densely populated Asian cities, where high spatial variability results from diverse local emission sources within communities (Kim et al., 2025; Lee et al., 2023; Lung et al., 2014).

However, most previous community $PM_{2.5}$ monitoring studies positioned LCSs at a height of 10 m to assess ambient levels, rather than at heights that accurately represent residents' actual exposure. Since public health concerns drive interest in $PM_{2.5}$ monitoring, measuring concentrations at street level is essential; accordingly, this study aimed to assess $PM_{2.5}$ concentrations at pedestrian height (2–3 m) to evaluate temporal and spatial variability and identify key exposure sources. Additionally, while most community monitoring studies conducted short-term observations spanning only weeks or months (Liu et al., 2020; Lung et al., 2020a; Zheng et al., 2018), our research presents findings from a nearly 3.5-year monitoring period—a duration rarely found in the existing literature. This long-term approach provides data that more accurately represents residents' chronic exposure patterns, offering valuable resources for environmental epidemiological studies investigating PM exposure-health relationships. Through this research, we demonstrate the significant advantages of sustained community monitoring and offer insights that can inform LCS deployment strategies in communities worldwide.

Materials and methods

Studied community

The studied community is within a town surrounded by mountains (Fig. S1(a)), situated at an elevation of approximately 150 m, with a size of roughly 1.5 km^2. Pollutants from Taiwan's western plain are frequently transported into this mountainous region where the surrounding topography restricts air circulation, resulting in pollutant accumulation, diminished air quality, and consequent health risks for residents. Beyond these external pollution sources, local emissions from vehicles, food vendors, and temples have also become a concern. The area surrounding the community is a popular tourist destination, experiencing a significant visitor influx, particularly during weekends.

The sensor network

In this study, we employed LCSs integrated and upgraded by Academia Sinica, called AS-LUNG-O, which were previously detailed in Lung et al. (2020a) and are briefly summarized here. Each AS-LUNG-O set incorporates a $PM_{2.5}$ sensor (PMS3003, Plantower, Beijing, China), a temperature and relative humidity sensor (SHT31, SENSIRION, Staefa ZH, Switzerland), a Secure Digital (SD) card, and a wireless transmission module. The system is solar-powered and operates at 1-min monitoring resolution. All AS-LUNG-O sets underwent chamber calibration against research-grade instruments—a GRIMM 1.109 (pre-2019) and an EDM-180 (post-2019), both from GRIMM Aerosol Technik GmbH & Co. KG (Ainring, Germany)—following protocols described in Wang et al. (2020b). The EDM-180 complies with the United States Environmental Protection Agency (USEPA) federal equivalent method (FEM). All measurements presented in this work have been converted to research-grade equivalents using calibration equations.

Ten AS-LUNG-O sets were deployed as an LCS network throughout the studied community in 2017 (Table 1). Nine AS-LUNG-O sets were mounted on street lamp posts at heights of 2.5 to 2.7 m, while one set was installed at approximately 12.5 m above ground inside a school, serving as a typical ambient (high-level) monitoring reference site. The street-level sets were strategically positioned 3–5 m from one or two PM emission sources, such as markets, vendors, traffic (categorized as stop-and-go or direct passage), and temples with incense-burning activities. Network monitoring commenced on December 1, 2017. The high-level measurements of $PM_{2.5}$ served as reference values against which other AS-LUNG-O readings were compared; incremental $PM_{2.5}$ levels above this reference were attributed to nearby source contributions. Data collection ended on July 8, 2021, when the school requested relocation of the high-level set, yielding approximately 3.5 years of monitoring data. During the monitoring period, regular checks and cleanings were conducted at intervals of once every 1 to 2 months.

Table 1 Features, heights, and monitoring durations of the AS-LUNG-O sets comprising the network

Location ID	Feature[a]	Height	Monitoring duration
H	High level	12.5 m	2017/12/1–2021/7/8
C-1	S, V_D	2.5 m	2017/12/1–2021/7/8
C-2	V_D	2.5 m	2017/12/1–2020/4/16
		2.7 m	2020/4/16–2021/7/8
C-3	M, V_D	2.5 m	2017/12/1–2021/3/9
		2.6 m	2021/3/9–2021/7/8
C-4	G, V_D	2.5 m	2017/12/1–2021/7/8
C-5	F, V_D	2.7 m	2017/12/1–2020/4/16
		2.5 m	2020/4/29–2021/7/8
C-6	T, V_SG	2.5 m	2017/12/1–2021/7/8
C-7	F, V_SG	2.5 m	2017/12/1–2021/7/8
C-8	T, V_SG	2.5 m	2017/12/1–2021/7/8
C-9	T, V_SG	2.5 m	2017/12/1–2021/7/8

[a]The street-level sensors were close to different sources, including F: fried chicken and other vendors; G: gasoline station; M: market; S: school; T: temple; V_D: emissions from passing vehicles; and V_SG: vehicle emissions from stop-and-go traffic

During the nearly 3.5 years of monitoring, the AS-LUNG-O sets at locations C-2, C-3, and C-5 were each relocated within a 100-m radius of their original locations due to safety concerns such as avoiding collisions with large vehicles while maintaining proximity to their designated emission sources (Fig. S1(b)). Data from before and after these relocations were integrated into our analysis.

The AS-LUNG-O sets were returned to the laboratory for chamber calibration at intervals of 1.5 to 2 years. The calibration curves obtained during the monitoring periods are presented in Supplementary Materials Table S1. Initially, linear regressions were used, but after October 2020, segmented regressions with two regions were applied based on our evaluation (Wang et al., 2020b). The coefficient of determination (R^2) for the calibration curves in this study ranged from 0.823 to 0.999 (Table S1). At the beginning of the study, R^2 values averaged 0.95 $\pm$0.04, with a maximum of 0.98 (Lung et al., 2020a). Following chamber calibration, the AS-LUNG-O sets were co-located with a GRIMM 1.109. The correlation between the calibration-adjusted readings from 10 AS-LUNG-O sets and GRIMM measurements, obtained at a 1-min resolution, was 0.93 $\pm$0.05 (Lung et al., 2020a), demonstrating the precision and accuracy of the AS-LUNG-O sets after calibration.

Moreover, inter-sensor variability was assessed in our chamber evaluation (Wang et al., 2020b). The percentage coefficient of variation (%CV), calculated as the standard deviation (SD) divided by the mean of the calibration curve slopes for 12 AS-LUNG-O sets, was 10.9%. When calibrated within the 0.1–200 μg/m^3 range, the average root mean square error was 2.4 $\pm$0.36 μg/m^3. To evaluate the repeatability of duplicate experiments, we used the intraclass correlation coefficient (ICC), a widely recognized reliability index for test–retest analyses (ranging from 0 to 1). The ICC for $PM_{2.5}$ calibration across the 12 AS-LUNG-O sets ranged from 0.988 to 0.998 (Wang et al., 2020b). Additionally, our previous evaluation indicated that sensor drift over 1.5 years was approximately 20% (Wang et al., 2020b).

Furthermore, one AS-LUNG-O set was not recalibrated over the 3.5-year period (Table S1). The R^2 values for regressions between data from this AS-LUNG-O and the nearest monitoring station of the Taiwan Ministry of Environment (TMOE), located 800 m away, ranged from 0.82 to 0.87 across different years (Fig. S2). Notably, these R^2 values showed no signs of degradation over time. The regression slopes varied between 0.65 and 0.85, indicating greater variability. The winter $PM_{2.5}$ maximum was 125.6, 137.8, 134.1, and 144.5 μg/m^3 in 2017, 2018, 2019, and 2020, respectively. Neither the regression slopes nor the maximum values exhibited a decreasing trend. Therefore, data from this AS-LUNG-O set remain included in the analysis and will be discussed later.

Additionally, Ouimette et al. (2024) reported that the Plantower 5003 sensor might be inefficient in capturing $PM_{2.5}$ at wind speeds exceeding 5 m/s. The AS-LUNG-O device, however, uses the Plantower 3003 sensor, which has a different inlet configuration. Moreover, during the 3.5-year monitoring period, only 0.23% of recorded wind speeds exceeded 3 m/s, and none surpassed 5 m/s. Therefore, no data were excluded due to concerns about wind speed.

For temperature and humidity sensors, Fig. S3(a), (b) presents the regression lines of the temperature and relative humidity, respectively, from the AS-LUNG-O set at high-level site and those from the co-located HOBO weather station (HOBO, RX3003, Onset, Bourne, MA, USA) during the monitoring period. The correlation is 0.999 for temperature and 0.91 for relative humidity, with slopes close to 1. The measurements of relative humidity exhibit more scattering than those of temperature, which is expected since relative humidity is a function of temperature. In short, these results demonstrate good data quality of temperature and humidity sensors.

Data analysis

The 1-min resolution measurements from the AS-LUNG-O sets were aggregated into hourly means for data presentation. After converting to research-grade measurements using calibration curves, the data underwent cleaning procedures to remove measurements from rainy days and “ghost peaks”—defined as instances where the $PM_{2.5}$ ratio for a given minute exceeded 10 times the average of the preceding and succeeding 5 min, potentially caused by spiders or small insects interfering with sensing components. Measurements showing abnormally high levels persisting over extended periods, indicative of sensor malfunctions, were also excluded. Meteorological parameters, including wind speed and direction, were collected from the HOBO weather station installed at the same high-level site (12.5 m above ground inside a school).

In this study, we compared $PM_{2.5}$ levels in three classifications: (1) warm (May to October) versus cold (November to April of the following year) seasons, (2) weekdays versus weekends, and (3) religious-event days versus typical days. The first two—cold versus warm seasons and weekdays versus weekends—were selected based on previous research demonstrating $PM_{2.5}$ concentration variations across seasons and days of the week in the same Taiwanese community (Lung et al., 2020a). The third classification focused on religious practices; due to the prevalence of Taoist and Buddhist traditions in Taiwan, burning incense and paper money is common in this community during the Lunar New Year days, as well as on the 1 st and 15 th days of lunar months. All other days were classified as typical days. GIS techniques were employed to identify hot spots with these classifications. Cases for each classification were selected for detailed illustration. Spatial variations in $PM_{2.5}$ were visualized using the inverse distance weighting (IDW, power = 2) spatial interpolation method using ArcGIS Pro 2.8.0.

Additionally, the contributions from different sources were evaluated using regression analysis, performed using RStudio version 2023.06.1 (RStudio, USA, 2023) and R version 4.3.1 (The R Foundation, Austria, 2023). Previous studies assessing various PM sources within communities were typically carried out using linear regression models (Franklin et al., 2012; Lung et al., 2014, 2020a; Zwack et al., 2011); however, in order to address the nonlinear relationships between $PM_{2.5}$ and meteorological variables (Hou & Xu, 2021) and the temporal autocorrelation in our data, we applied a generalized additive mixed model (GAMM) to evaluate the relationships between environmental factors and $PM_{2.5}$ (Song et al., 2015; Tsou et al., 2021a, b). Additionally, collinearity was checked using a variance inflation factor (VIF) with a threshold of 3 (Li et al., 2021; Wolf et al., 2017; Xu et al., 2019). The GAMM is listed as follows:

$$P_{\text{location}} = \beta 0 + \gamma_1 P_{\text{high-level}} + \gamma_2(\text{RH}) + \gamma_3 Ws + \sum \beta_{\text{i}} X_{\text{i}} + s(Time) + \varepsilon \quad (1)$$

P_{location} represents the hourly mean of observed $PM_{2.5}$ at the street levels, while $P_{\text{high-level}}$ denotes the corresponding hourly mean observed at the high-level site. $\beta 0$ is the intercept; $\gamma_1, \gamma_2, \gamma_3$, and β_{i} are regression coefficients; ε is the error term. RH refers to the hourly mean of the relative humidity measured at each location. Due to collinearity between relative humidity and temperature, our model adjusts for relative humidity rather than temperature. *Ws* represents hourly wind speed (meters per second) collected from the HOBO weather station. A smoothing term, *s*, was incorporated into the model using cubic regression splines to address non-linear temporal relationships. Additionally, a first-order autoregressive model (AR(1)) was implemented to eliminate temporal autocorrelation for each location.

X_{i} represents dummy variables addressing three different aspects: PM sources, wind directions, and other time-related adjustment factors. PM sources included emissions from passing vehicles, stop-and-go traffic, gas stations, street vendors, elementary schools, markets, and temples. The dummy variable for each source was assigned 1 during active periods and 0 during inactive periods. Most emission sources exhibited reduced activity during nighttime. Traffic was considered active from 6:00 to 22:00 daily; gas stations from 7:00 to 22:00; street vendors or restaurants typically from 17:00 to 23:00 daily, excluding closure days. Elementary school activity periods were defined as 7:00–8:00 and 16:00–17:00 on regular school days, when parents gathered with vehicles to drop off and pick up children, plus 12:00–13:00 for lunch delivery, with summer and winter breaks designated as inactive periods. The local market primarily operated in the evening, with activity defined from 14:00 to 19:00 daily. Incense-burning activities in temples were considered active from 7:00 to 22:00 daily. During the model evaluation process, the dummy variables of the gas station and the temple were removed due to collinearity concerns.

The second aspect of X_{i} relates to wind direction, with north wind (> 315°, ≤45°) established as the reference class. Other classes include east (> 45°, ≤135°), south (> 135°, ≤225°), and west (> 225°, ≤315°) winds. When the prevailing wind direction fell within a specific range during a given hour, the corresponding dummy was assigned a value of 1.

The third aspect comprised additional time-related adjustment variables, including days of the week, lunar event days, and the COVID-19 pandemic period. Monday served as the reference for weekday comparisons. The 1 st and 15 th days of each lunar month, along with the Lunar New Year festival days, were designated as religious events. For the COVID-19 pandemic variable, Taiwan's lockdown period from May 19 th to July 26 th, 2021 (Ministry of Health & Welfare, 2021) was included, during which all emission sources exhibited reduced activity.

To further assess spatial variation across different locations, the same model was run for each location. These individual-location models did not include dummy variables if the corresponding sources were not in the surrounding area. The rest of the settings were the same as the main model.

Results and discussion

PM distribution among different locations

Table 2 presents the distributions of hourly $PM_{2.5}$ concentrations across 10 locations during the 3.5-year monitoring period. The $PM_{2.5}$ levels at the high-level site were 18.8 ±9.7 μg/m^3, with a maximum of 83.3 μg/m^3. The mean hourly $PM_{2.5}$ concentrations across all street-level locations were 24.3 ±14.1 μg/m^3. Most street-level locations demonstrated higher mean and maximum $PM_{2.5}$ levels compared to the high-level site, with one notable exception: location C-4, situated near a gasoline station with frequent vehicle traffic. This location had mean $PM_{2.5}$ levels of 18.8 ±12.0 μg/m^3, showing minimal differences from the high-level site but with significantly greater variability. The location's positioning at an intersection with intermittent high wind speeds likely contributed to its comparatively lower $PM_{2.5}$ levels relative to other street-level locations.

Location C-6, situated near a temple, had the highest mean $PM_{2.5}$ concentrations at 32.9 ±17.4 μg/m^3, with a maximum of 144.5 μg/m^3. A previous study in the same community reported hourly $PM_{2.5}$ concentrations at location C-6 of 22.0 ±12.2 μg/m^3 in July 2017 and 48.0 ±25.9 μg/m^3 in December 2017 (Lung et al., 2020a). In the current study, the overall concentrations of nine street-level locations during the warm season (17.4 ±10.4 μg/m^3) closely aligned with the previous results (18.1 ±9.6 μg/m^3) after just 1 month of monitoring. Conversely, the concentrations for the same nine street-level locations during the cold season (30.0 ±14.3 μg/m^3) were lower than those in the previous 1-month monitoring period (37.8 ±20.7 μg/m^3). The discrepancy may be attributed to the previous study's monitoring period coinciding with a religious event involving nearly month-long incense and paper money burning, which was not held regularly every year.

A previous study conducted in a semi-open temple in central Taiwan reported a mean $PM_{2.5}$ concentration of 75.1 μg/m^3 over 39 days from August 2001 to January 2002, with monitoring between 9:00 and 19:00 (Fang et al., 2003), substantially higher than our findings. Several potential factors may explain this discrepancy: first, variations in temple size, worshipper numbers, and sampling durations could contribute to the difference. Second, the Taiwanese government has implemented a nationwide initiative since the 2010s to reduce incense stick usage from three to one per censor, resulting in decreased incense burning, which is reflected in our results. Third, strict environmental policy implementation in Taiwan in recent years may have contributed to overall air quality improvements (Chen et al., 2014; Chou et al., 2023). In summary, these factors likely account for the disparities in $PM_{2.5}$ mean concentrations observed across different temple studies in central Taiwan.

Table 2 Hourly $PM_{2.5}$ levels (μg/m^3) among different locations during the 3.5-year monitoring period

Location	Feature[a]	Mean (SD)	Maximum	Correlation[b]	Sample size
H	High-level	18.8 (9.7)	83.3	0.825	28,328
C-1	S, V_D	22.5 (11.2)	139.7	0.875	28,017
C-2	V_D	22.2 (12.5)	98.1	0.851	14,896
C-3	M, V_D	26.9 (14.9)	123.9	0.855	15,702
C-4	G, V_D	18.8 (12.0)	165.4	0.766	27,234
C-5	F, V_D	24.2 (11.8)	118.0	0.830	18,585
C-6	T, V_SG	32.9 (17.4)	144.5	0.860	26,057
C-7	F, V_SG	19.5 (13.5)	115.6	0.781	27,677
C-8	T, V_SG	24.4 (11.9)	110.9	0.866	27,763
C-9	T, V_SG	27.5 (14.6)	128.1	0.867	28,656
TMOE	High-level	23.5 (16.0)	135.0	–	30,268

[a]The street-level sensors were close to different sources, including F: fried chicken and other vendors; G: gasoline stations; M: markets; S: schools; T: temples; V_D: emissions from passing vehicles; and V_SG: emissions from stop-and-go traffic

[b]Correlation with $PM_{2.5}$ of the nearest monitoring station of the Ministry of the Environment, Taiwan (TMOE)

The nearest monitoring station of the Ministry of the Environment, Taiwan (TMOE) is only 640 m from our high-level site. Thus, the observations from that station were compared with those of the AS-LUNG-O sets; the mean and maximum $PM_{2.5}$ concentrations at the TMOE station are all within the ranges of the measurements from the AS-LUNG-O sets during the monitoring period. The AS-LUNG-O measurements at all locations have good correlations (0.766 to 0.875) with the observations of the TMOE station.

PM distributions among different classifications

The means and SDs of $PM_{2.5}$ levels during the 3.5-year monitoring period are shown in Fig. 1, with three classifications: (1) cold versus warm seasons, (2) weekdays versus weekends, and (3) religious-event days versus typical days. Regarding seasonal differences, the $PM_{2.5}$ concentrations were higher during the cold season compared to the warm season (Fig. 1a). In addition, the $PM_{2.5}$ levels at each station appeared to be slightly higher on weekends than on weekdays (Fig. 1b); this weekday–weekend discrepancy may be attributed to increased traffic emissions, resulting from an influx of tourists during weekends. Moreover, $PM_{2.5}$ levels were higher during religious-event days than on typical days (Fig. 1c). The impacts of burning incense and paper money affected not only the neighborhoods near temples but also the entire community. Location C-6 is near a famous temple; thus, the incremental increase on religious-event days compared to typical days was higher than those at other locations (Fig. 1c).

The maximum $PM_{2.5}$ concentrations during the entire monitoring period are listed in Table 3. Most locations exhibited higher $PM_{2.5}$ maxima during cold seasons compared to warm seasons (Table 3(a)). Contrary to expectations, maximum $PM_{2.5}$ levels at most locations were higher on weekdays than on weekends, with a few exceptions (Table 3(b)). Location C-5, situated near a fried

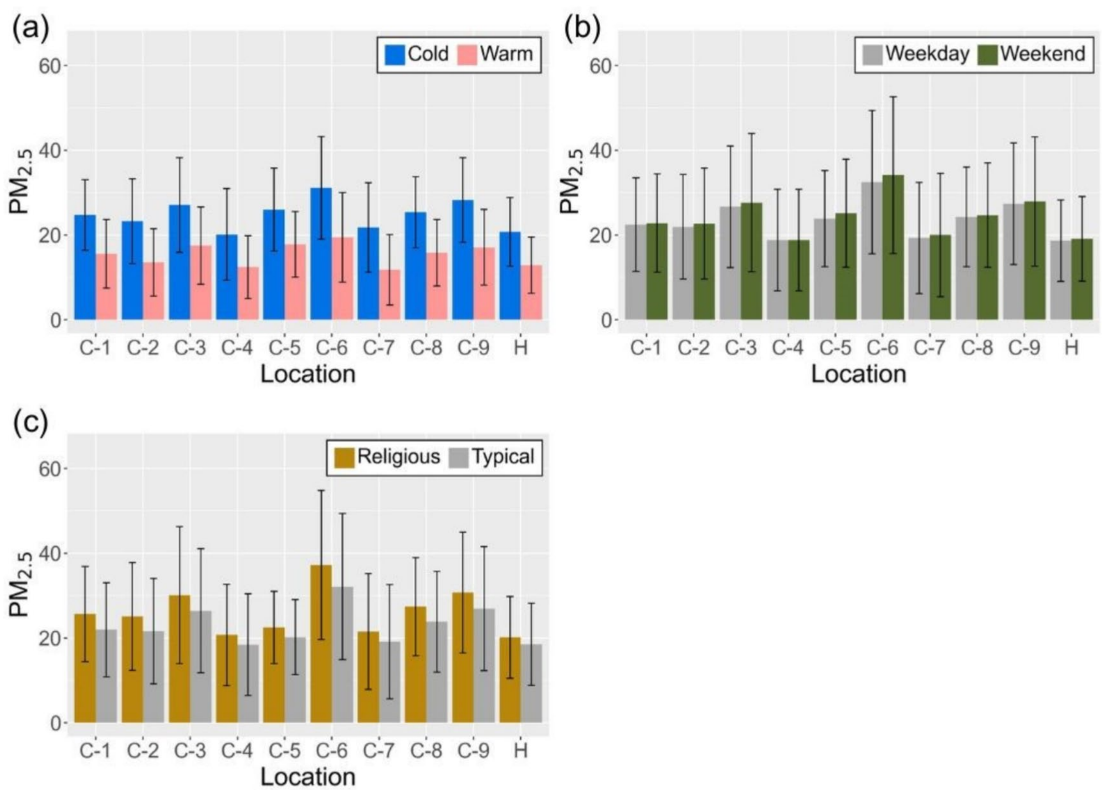

Fig. 1 Mean $PM_{2.5}$ concentrations (μg/m^3) at each location, based on different classifications. **a** Warm and cold seasons, **b** weekdays and weekends, and **c** religious-event and typical days. The black lines on the bars indicate plus or minus one SD

chicken vendor, stood out as a notable exception, showing higher maximum $PM_{2.5}$ levels on weekends compared to weekdays. Furthermore, maximum $PM_{2.5}$ levels at most locations during typical days exceeded those on religious-event days (Table 3(c)). These unexpected findings indicate the unpredictable nature of street-level source emissions in the community. Our long-term monitoring approach uniquely captured high $PM_{2.5}$ levels from irregular and unexpected emissions, which would have been overlooked in short-term monitoring.

To illustrate $PM_{2.5}$ levels elevated above the daily background concentration, we calculated the ratio of daily PM maximum to the daily background concentration (22:00 to 05:59 of the following day) for each location across three classifications (Table 3). The means of these ratios reveal the typical $PM_{2.5}$ difference between daily maximum and background periods. Across all classifications, daily maximum $PM_{2.5}$ levels typically exceeded 30–50% of daily background levels, with some instances reaching 60–80%. Unlike the maximum $PM_{2.5}$ concentration patterns, most ratios in the cold season were similar to or lower than those in warm seasons, with location C-2 (affected by passing vehicle emissions) being the primary exception (Table 3(a)). The highest $PM_{2.5}$ ratios (1.7 $\pm$ 1.1) were observed at location C-6 near a temple during warm seasons. These divergent patterns of maxima and average max/background ratios over the 3.5-year monitoring period demonstrate the significant variability in source emissions.

Analyzing the relative magnitudes of $PM_{2.5}$ maxima and maximum/background ratios between weekends and weekdays revealed different patterns. While weekend ratios were similar to or slightly higher than weekday ratios, this contrasted with the maxima, which were predominantly higher on weekdays. Location C-6 (near a temple) exhibited the highest maximum/background ratio of 1.6 for $PM_{2.5}$ (Table 3(b)). The substantial sample sizes for both weekend and weekday monitoring enhance the representativeness of the results. Interestingly, the data suggest two seemingly contradictory observations: PM levels elevated above background were generally higher on weekends, yet the peak levels captured by long-term monitoring occurred predominantly on weekdays. These findings further underscore the complex and unpredictable nature of source emissions at the community street level.

Table 3 The maximum $PM_{2.5}$ concentrations (μg/m^3) over the entire monitoring period, and the mean (and SD) of the ratios of the daily $PM_{2.5}$ maxima over the daily background levels (22:00 to 05:59 of the following day) in different categories: (a) cold versus warm seasons, (b) weekdays versus weekends, and (c) religious-event days versus typical days

Location	Category	Maximum (μg/m^3)	Maximum/background mean (SD)	Sample size
(a) Cold versus warm seasons				
H	Cold	83.3	1.3 (0.3)	14,914
	Warm	82.3	1.3 (0.3)	13,414
C-1	Cold	98.7	1.4 (0.5)	14,644
	Warm	139.7	1.5 (0.6)	13,373
C-2	Cold	98.1	1.5 (0.8)	9,120
	Warm	70.5	1.4 (0.4)	5,776
C-3	Cold	123.9	1.4 (0.4)	8,173
	Warm	100.7	1.5 (0.6)	7,529
C-4	Cold	165.4	1.4 (0.7)	14,718
	Warm	71.6	1.4 (0.4)	12,516
C-5	Cold	118.0	1.5 (0.6)	8,911
	Warm	71.0	1.5 (0.5)	9,674
C-6	Cold	144.5	1.5 (0.4)	16,367
	Warm	96.2	1.7 (1.1)	9,690
C-7	Cold	115.6	1.4 (0.4)	15,029
	Warm	80.8	1.5 (0.5)	12,648
C-8	Cold	110.9	1.4 (0.4)	15,048
	Warm	78.0	1.5 (0.5)	12,715
C-9	Cold	128.1	1.4 (0.4)	15,320
	Warm	96.7	1.4 (0.6)	13,336
(b) Weekdays versus weekends				
H	Weekday	83.3	1.3 (0.3)	20,189
	Weekend	79.1	1.4 (0.3)	8,139
C-1	Weekday	139.7	1.4 (0.6)	19,930
	Weekend	82.5	1.4 (0.4)	8,087
C-2	Weekday	98.1	1.4 (0.7)	10,584
	Weekend	87.7	1.5 (0.5)	4,312
C-3	Weekday	118.4	1.5 (0.5)	11,170
	Weekend	123.9	1.5 (0.5)	4,532
C-4	Weekday	165.4	1.4 (0.4)	19,420
	Weekend	122.7	1.5 (0.9)	7,814
C-5	Weekday	99.5	1.5 (0.4)	13,260
	Weekend	118.0	1.5 (0.7)	5,325
C-6	Weekday	144.5	1.6 (0.8)	18,551
	Weekend	128.4	1.6 (0.6)	7,506
C-7	Weekday	115.6	1.4 (0.4)	19,827
	Weekend	104.2	1.4 (0.5)	7,850
C-8	Weekday	110.9	1.4 (0.4)	19,778
	Weekend	87.6	1.5 (0.5)	7,985

Table 3 (continued)

Location	Category	Maximum (μg/m^3)	Maximum/background mean (SD)	Sample size
C-9	Weekday	128.1	1.4 (0.5)	20,470
	Weekend	111.9	1.4 (0.5)	8,186
(c) Religious-event days versus typical days				
H	Religious	67.3	1.3 (0.2)	4,179
	Typical	83.3	1.3 (0.3)	24,149
C-1	Religious	139.7	1.4 (0.6)	4,362
	Typical	98.7	1.4 (0.5)	23,655
C-2	Religious	75.0	1.4 (0.3)	2,417
	Typical	98.1	1.4 (0.7)	12,479
C-3	Religious	110.8	1.5 (0.5)	2,247
	Typical	123.9	1.5 (0.5)	13,455
C-4	Religious	91.9	1.4 (0.3)	4,243
	Typical	165.4	1.4 (0.6)	22,991
C-5	Religious	118.0	1.5 (0.3)	2,702
	Typical	112.0	1.5 (0.4)	15,883
C-6	Religious	134.1	1.8 (1.3)	4,135
	Typical	144.5	1.6 (0.6)	21,922
C-7	Religious	96.6	1.4 (0.4)	4,097
	Typical	115.6	1.4 (0.4)	23,580
C-8	Religious	84.1	1.5 (0.5)	4,249
	Typical	110.9	1.4 (0.4)	23,514
C-9	Religious	106.4	1.4 (0.5)	4,342
	Typical	128.1	1.4 (0.5)	24,314

Regarding religious activities, most maximum/background ratios during religious-event days were similar to or slightly higher than those on typical days, with a notable exception at location C-6 (Table 3(c)). The proximity of temples near location C-6 substantially influenced $PM_{2.5}$ levels, resulting in significantly elevated concentrations relative to background levels during religious-event days. The average maximum/background ratio at location C-6 was 1.8 for $PM_{2.5}$ on religious-event days, compared to 1.6 on typical days—both the highest among all monitored locations. Consistently, the maximum/background ratios at location C-6 across all three classifications remained higher than those observed at other locations.

Hot spot identification

Subsequently, we identified $PM_{2.5}$ hotspots across different classifications. To compare hotspots between cold and warm seasons, we selected cases at noon on Mondays—one in each season—carefully chosen to avoid religious-event days and the COVID-19 pandemic period. Figure 2a presents a snapshot of hourly $PM_{2.5}$ at noon on January 21, 2019 (cold season), which is compared with the warm-season case at noon on September 30, 2019 (Fig. 2b). The spatial distribution's color gradient was categorized based on the observed values in each snapshot to emphasize $PM_{2.5}$ hotspots within the community. The hourly mean $PM_{2.5}$ concentration differed markedly between these cases, measuring 33.0 μg/m^3 in the cold-season snapshot and 19.3 μg/m^3 in the warm-season snapshot.

In the cold-season case, locations C-3 (market and passing vehicle emissions), C-6 (temple and stop-and-go traffic emissions), and C-9 (temple and stop-and-go traffic emissions) emerged as hotspots, with $PM_{2.5}$ levels reaching approximately 40 μg/m^3. During the warm-season case, locations C-3 and C-6 remained hotspots, with $PM_{2.5}$ levels around 30 μg/m^3, while C-9 no longer appeared as a hotspot. These observations suggest that the distribution of pollution hotspots within the community can be dynamic and seasonally variable.

To assess hotspot variations between weekdays and weekends, we selected two cases for comparison. Figure 3a, b reveals that the hotspots on Monday and Saturday within the same week exhibited subtle differences. The $PM_{2.5}$ concentrations on Saturday, with a mean of 38.8 μg/m^3, were substantially higher than Monday's mean of 16.8 μg/m^3. On Monday, locations C-3, C-6, and C-9 were identified as hotspots. In contrast, Saturday's pattern showed locations C-6 and C-9 remained hotspots, while C-3 was no longer prominent. Additionally, location C-7 (characterized by stop-and-go traffic emissions) emerged as a minor PM hotspot on Saturday.

Moreover, two cases were selected to evaluate the hotspots on religious-event days, as opposed to typical days. The spatial distribution of $PM_{2.5}$ on the first day of the 2019 Lunar New Year (Fig. 4a) was compared with the $PM_{2.5}$ distribution 6 weeks later (Fig. 4b). On the Lunar New Year, $PM_{2.5}$ levels ranged from 37.5 to 69.3 μg/m^3, with a mean of 49.4 μg/m^3. Six weeks

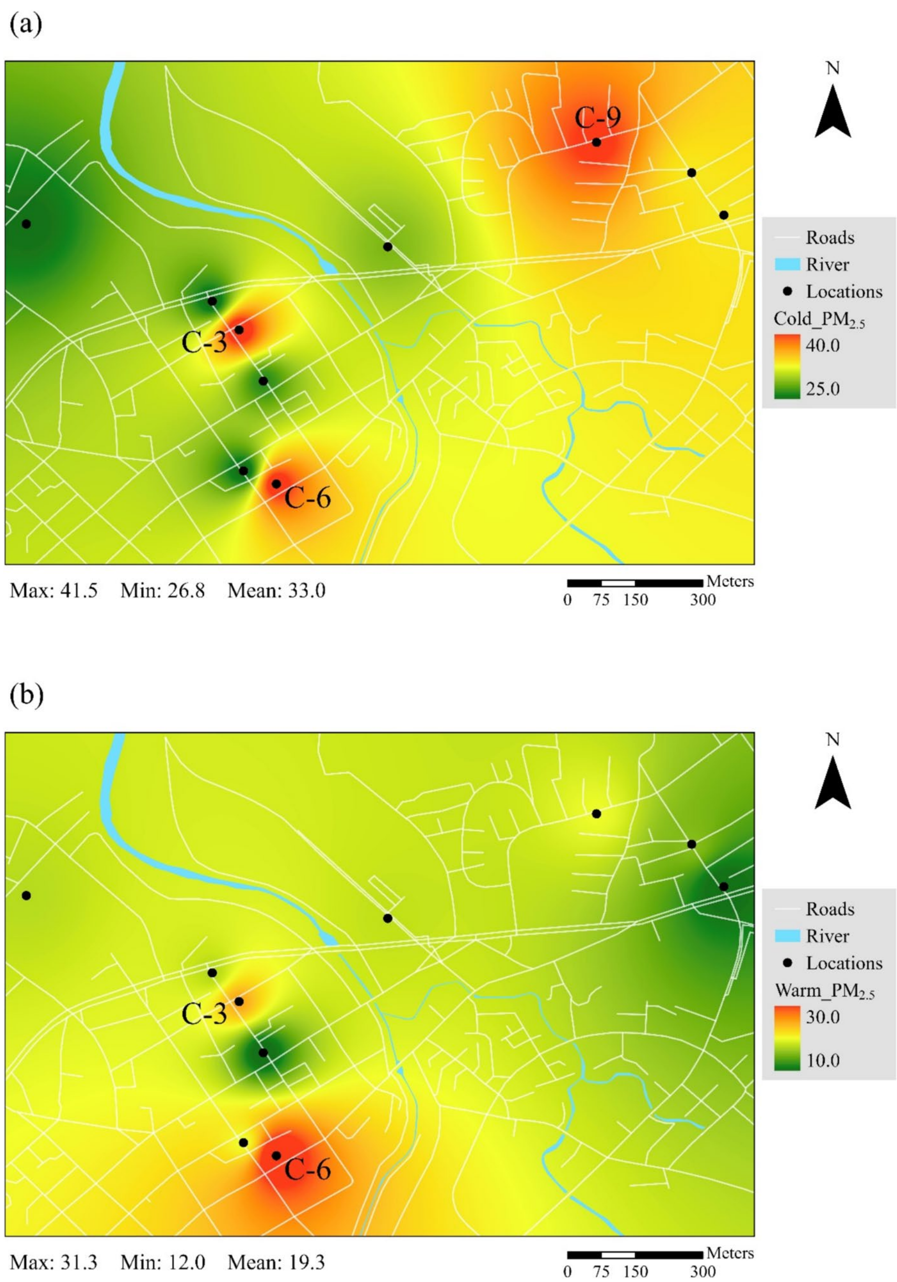

Fig. 2 The spatial distributions of the hourly mean $PM_{2.5}$ concentrations (μg/m^3) among the 10 locations at **a** 12:00 on January 21, 2019 (Monday), with an hourly temperature of 16.7 °C (cold-season case) and **b** 12:00 on September 30, 2019 (Monday), with an hourly temperature of 29.4 °C (warm-season case)

later, levels ranged from 23.3 to 41.2 μg/m^3, with a mean of 29.6 μg/m^3. The worshipping traditions and fireworks associated with the Lunar New Year visibly elevated $PM_{2.5}$ levels across the entire community. In terms of hotspot analysis, locations C-6 and C-9, both situated near temples, remained hotspots in both cases. Location C-7 showed slightly elevated $PM_{2.5}$ levels on religious-event days, whereas location C-3 emerged as a hotspot on typical days.

Based on the above hotspot analysis, location C-6, near a religious center, was predominantly identified as a hotspot regardless of different classifications; the nearby temple attracts both local residents and tourists engaging in incense and paper money burning—a practice that substantially contributes to $PM_{2.5}$ pollution. Locations C-3 (market and passing vehicle emissions), C-7 (stop-and-go traffic emissions), and C-9 (temple and stop-and-go traffic emissions)

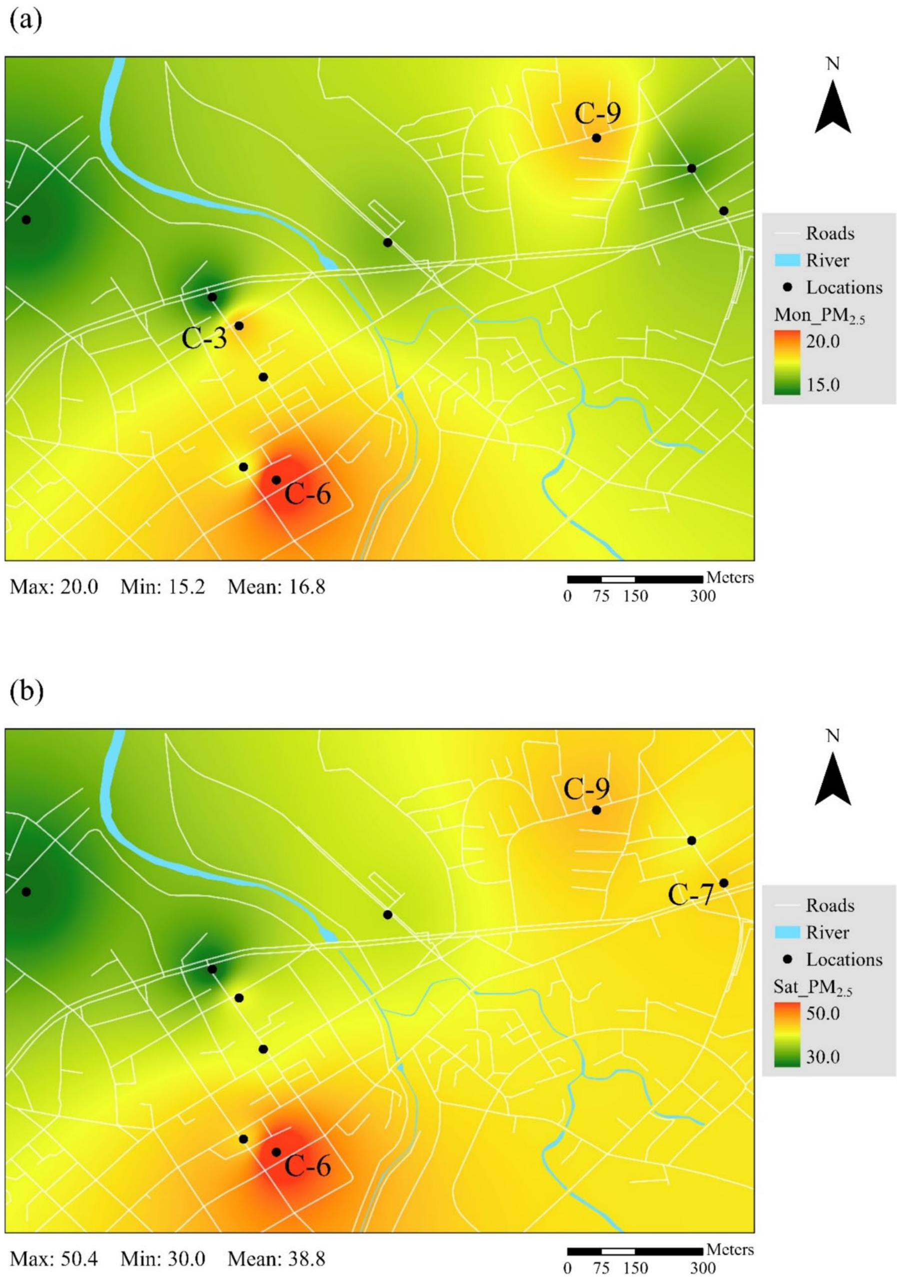

Fig. 3 The spatial distributions of the hourly mean $PM_{2.5}$ concentrations (μg/m^3) at **a** 12:00 on August 6, 2018 (Monday) and **b** 12:00 on August 11, 2018 (Saturday)

were also identified as $PM_{2.5}$ hotspots in the selected cases. Nevertheless, the intensity of nearby emission sources appeared to fluctuate over time, resulting in these locations not consistently qualified as hotspots.

In summary, our spatial distribution analyses unveiled $PM_{2.5}$ hotspots across various classifications, revealing the dynamic nature of $PM_{2.5}$ emission sources. The findings highlight the variability in $PM_{2.5}$ distribution across different locations and underscore the critical role of local emission sources, such as temples and markets, in understanding community-level $PM_{2.5}$ exposure.

Source contributions

The determinants of the hourly $PM_{2.5}$ levels at the street level over the studied 3.5-year monitoring period were evaluated using regression analysis

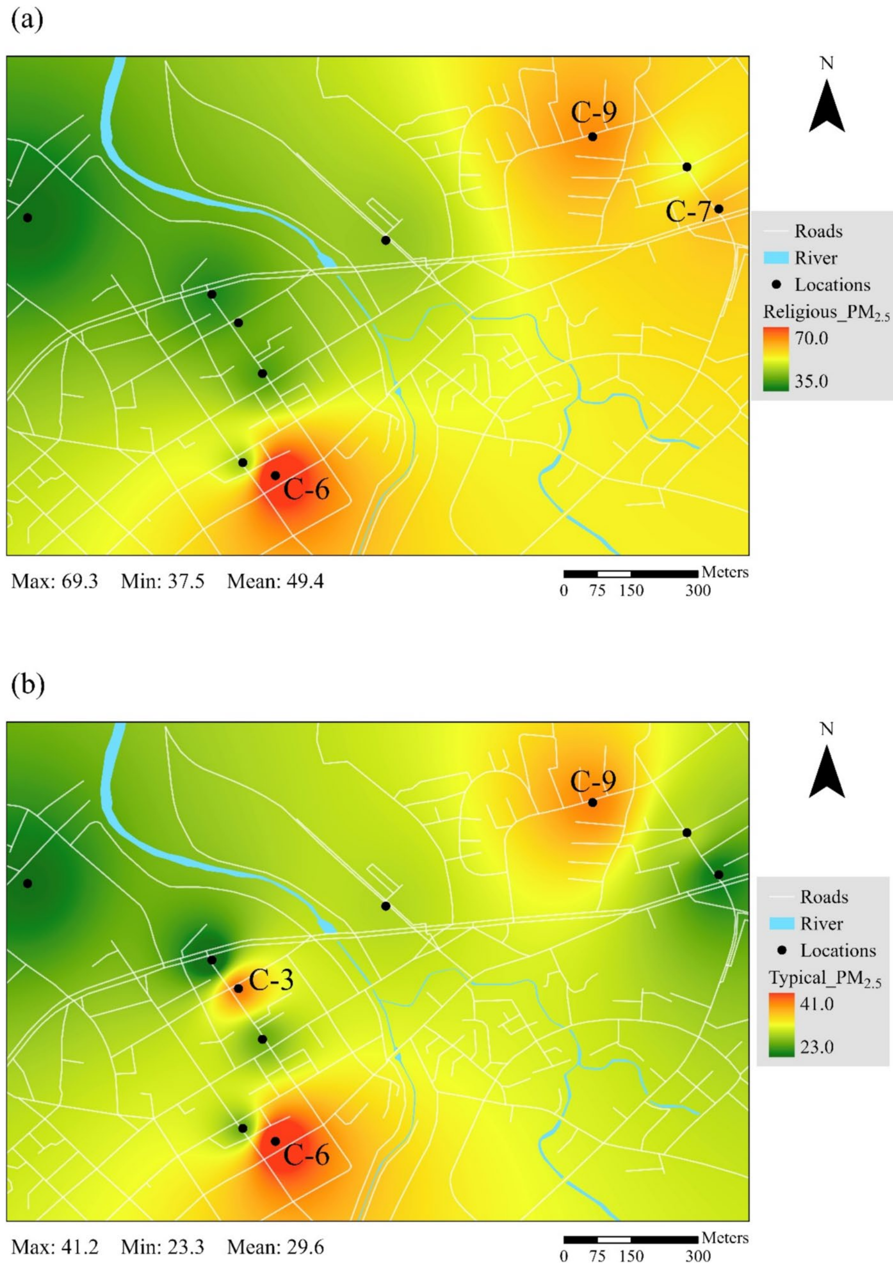

Fig. 4 The spatial distributions of the hourly mean $PM_{2.5}$ concentrations (μg/m.^{3}) at **a** 12:00 on February 5, 2019 (Lunar New Year's Day, Tuesday) and **b** 12:00 on March 19, 2019 (6 weeks later, Tuesday)

(Table 4). Religious events emerged as the most significant factor influencing community $PM_{2.5}$ concentrations, aligning with the hotspot analysis that consistently identified the location near a famous temple (C-6) as a prominent hotspot. The estimated incremental hourly contribution from religious events was 2.05 μg/m^3. Traditional practices of burning incense and paper money at temples and homes during major lunar festivals, as well as on the 1st and 15th days of lunar months, statistically significantly elevated street-level $PM_{2.5}$ concentrations within the community. Vendors ranked as the second most influential source, contributing approximately 0.30 μg/m^3 to hourly $PM_{2.5}$ levels.

Meteorological factors played a significant role in determining PM concentrations within the studied community, with relative humidity, wind speed, and wind direction emerging as key factors. As expected,

Table 4 The coefficient estimates of various determinants on hourly $PM_{2.5}$ levels within the studied community for the main model with nine locations as a whole (adj. $R^2 = 0.682$, $n = 197{,}703$)

Parameter		Coefficient estimate (μg/m³)	Standard error	p-value
Intercept		− 0.86	0.15	< 0.001
High-level site		1.06	0.00	< 0.001
Relative humidity		0.06	0.00	< 0.001
Wind speed		− 0.32	0.02	< 0.001
Wind direction	East	0.22	0.02	< 0.001
	West	0.06	0.02	0.001
	South	0.33	0.03	< 0.001
Traffic	Passing	0.02	0.04	0.615
	Stop-and-go	0.16	0.04	< 0.001
Feature	School	0.15	0.06	0.009
	Vendors	0.30	0.06	< 0.001
	Market	− 0.05	0.09	0.564
Religious event		2.05	0.18	< 0.001
Weekend		0.05	0.05	0.307
Pandemic shutdown		− 9.11	0.38	< 0.001

higher relative humidity was associated with increased $PM_{2.5}$ levels, given that water droplets are classified as aerosols by definition. In contrast, higher wind speeds correlated with lower PM concentrations. Wind direction analysis indicated that eastern, western, and southern winds led to slightly elevated $PM_{2.5}$ levels compared to northern winds.

Moreover, government-imposed lockdown measures during the COVID-19 pandemic restricted public activities, leading to a reduction in $PM_{2.5}$ concentrations by 9.11 μg/m³ within the community (Table 4). Regression analysis for individual locations further highlights spatial variations across different locations (Table 5). The impact of COVID-19 on $PM_{2.5}$ reductions ranged from 10.7 to 15.2 μg/m³, indicating an even greater decrease than the main model suggested. These reductions exceed those previously reported for ambient $PM_{2.5}$ levels. Prior studies found that $PM_{2.5}$ concentrations declined from 18.0 ± 6.1 to 15.0 ± 7.0 μg/m³ based on data from 69 Taiwan EPA monitoring stations across the island (Latif et al., 2024; Wong et al., 2022).

Certain variables that are not statistically significant in the main model become statistically significant at certain locations (Table 5). For example, the traffic emissions of passing vehicles contribute statistically significantly to locations C-1, C-3, and C-4, ranging from approximately 0.26 to 0.64 μg/m³. The contribution of vendors to C-5 is 0.46 μg/m³, which is slightly higher than the estimate in the main model. The most surprising results are the coefficient estimates for religious events, which range 2.86 to 6.07 μg/m³ for all locations, higher than the estimate of the main model. C-6, near a temple, have the highest contribution. Due to concerns about collinearity, the variable "temple" was removed from the model. However, the contribution of burning incenses and paper money is shown in the variable of the religious event.

In comparison to short-term monitoring (Lung et al., 2020a), our long-term monitoring shows fewer significant contributing pollution sources in the main model. This difference stems from the smoothing effect of extended observations, which reduces the impact of isolated high-pollution events. In contrast, short-term monitoring typically emphasizes specific high-pollution incidents, potentially overestimating source contributions and introducing biases when extrapolating these results as representative exposure levels for local residents in environmental epidemiology. Long-term monitoring provides more representative exposure assessments, offering crucial insights into community air quality trends and identifying persistent sources of PM pollution that continually influence local environmental conditions.

Table 5 The coefficient estimates of various determinants on hourly $PM_{2.5}$ levels within the studied community for the models for individual locations

Location	Traffic		Feature			Religious event	Weekend	Pandemic shutdown
	Passing	Stop-and-go	School	Vendors	Market			
C-1	0.37***	–[a]	0.20**	–	–	4.03***	0.06	− 13.9***
C-2	0.12	–	–	–	–	3.39**	0.02	− 10.7***
C-3	0.64***	–	–	–	− 0.17	4.84***	0.20	NA[b]
C-4	0.26*	–	–	–	–	2.86***	0.03	− 13.6***
C-5	0.29	–	–	0.46***	–	5.47***	0.59**	− 14.7***
C-6	–	0.53*	–	–	–	6.07***	0.26	NA[b]
C-7	–	0.36**	–	− 0.02	–	3.37***	− 0.06	− 13.7***
C-8	–	0.55***	–	–	–	4.55***	0.01	− 13.9***
C-9	–	0.21	–	–	–	4.55***	0.32	− 15.2***

***: $p < 0.001$; **: $0.001 < p < 0.01$; *: $0.01 < p < 0.05$

[a]No such a source at that location

[b]Sensor not in use during that period

Overall discussion

LCS development has increasingly sparked interest in community air quality monitoring, as summarized in Table S2. Previous studies' monitoring durations ranged from several days to a year, with one notable exception—a 3-year study in Greece by Kosmopoulos et al. (2022). In that study, 16 LCS sets monitored urban air quality, revealing distinct pollution source variations between warm and cold seasons. Our current study, which conducted street-level community monitoring over three and a half years, represents the longest monitoring period among comparable existing studies. Earlier campaigns lacked sufficient sample sizes to comprehensively assess $PM_{2.5}$ level variations across seasons, weekdays versus weekends, and religious events versus typical days. Our extended monitoring approach offers an unprecedented opportunity to comprehensively evaluate temporal trends, identify pollution hotspots, and assess contributions from various sources to community $PM_{2.5}$ levels. The resulting scientifically valid conclusions can be drawn with greater confidence. Moreover, these extensive monitoring observations offer valuable insights for environmental epidemiological studies, enabling more accurate health impact assessments without the risk of overestimation. Our work demonstrates that research-grade AS-LUNG-O sets can effectively complement traditional monitoring stations of the authorities. Given that LCS sets represent a relatively affordable monitoring tool, strategically deployed LCS networks can assess long-term $PM_{2.5}$ concentrations in polluted or underserved neighborhoods.

Examining concentration levels from literature, most studied communities reported $PM_{2.5}$ levels below 30 μg/m^3 (Table S2). Some studies are with $PM_{2.5}$ levels above 30 μg/m^3. For example, daily $PM_{2.5}$ levels were observed during the heating season in Italy (Gualtieri et al., 2024), with $PM_{2.5}$ concentrations up to 60 μg/m^3. Daily $PM_{2.5}$ levels were up to 80 μg/m^3 in Bandung, Indonesia, due to traffic and intensive industrial activities (Kurniawati et al., 2025). Another example is India, where mean levels ranged from 28 to 137 μg/m^3 due to the influence of the monsoon climate, which facilitates the transport of dry dust particles from arid regions (Chaudhry et al., 2024; Zheng et al., 2018). Similar to those studies, our community experiences transported pollution during cold seasons, though our long-term average $PM_{2.5}$ levels across ten locations remained below 35 μg/m^3 (i.e., 24-h $PM_{2.5}$ standard in Taiwan, Fig. 1a). In general, the $PM_{2.5}$ concentrations recorded during our 3.5-year monitoring period were within the range reported in earlier studies, as detailed in Table S2.

Existing literature highlights diverse $PM_{2.5}$ sources across different communities. Some studies have identified heavy industrial activities (Tseng et al., 2021; Zheng et al., 2018) or coal-fired power plants (Kim et al., 2025) as primary contributors to urban $PM_{2.5}$ levels, while others noted biomass burning for residential heating during winter months as a major source of organic aerosols in regions like Patras, Greece (Kosmopoulos et al., 2022). Religious practices have also emerged as significant $PM_{2.5}$ contributors in multiple studies (Lee et al., 2024; Lung et al., 2020a). Consistent with these findings, our study identified traffic, religious practices (specifically incense and paper money burning), and vendors as key sources contributing to $PM_{2.5}$ levels in the studied community.

The advantage of using green energy (solar panels) as the power supply for the AS-LUNG-O is that it provides the flexibility of setting up sensors in any place with sunshine with much lower operation expenses than traditional monitoring stations, which even require air-conditioning rooms. Our 3.5-year long-term monitoring largely confirmed the community sources identified in earlier analyses focused on month-long observations in summer and winter 2017, though source contribution estimations showed variations. The large sample size obtained in long-term monitoring offers more representative measurements for residents' actual PM exposure at the street level. On the other hand, AS-LUNG-O requires regular maintenance, including cleaning, replacing malfunctioning sensors, and checking the time settings; thus, it still requires manpower and resources for operation.

Numerically, the incremental increase of 2.86–6.07 μg/m^3 attributed to religious events may appear small; however, its potential health impacts remain a concern. These findings show that religious events have statistically significant impacts on the whole community, not just in the surrounding of the temples. And repeated exposure to the enhanced $PM_{2.5}$ levels twice every month plus several important culture festivals may lead to health concerns. Our previous works showed that healthy adults had reduced heart rate variability (HRV) immediately right after $PM_{2.5}$ exposure (Lung et al., 2020b), and reduced HRV was associated with an increased risk of myocardial infarction (Sinnreich et al., 1998). It was found that an increase of 10 μg/m^3 in $PM_{2.5}$ was statistically significantly associated with reduced 3.44% (CI = 2.86–4.01%) of the SD of normal-to-normal intervals (SDNN) of heart rates in 36 non-smoking healthy subjects aged 20–65 in Taiwan in 2017–2018, in the concentration ranges of 12.6 ± 8.9 μg/m^3 which was below the 24-h $PM_{2.5}$ standard in Taiwan (35 μg/m^3). In other words, even in such low $PM_{2.5}$ levels, immediate changes in the HRV of the subjects were evident. In this work, a 6.07 μg/m^3 increase in $PM_{2.5}$ at C-6 may result in a 2.1% reduction of the SDNN, according to our previous findings. Moreover, these AS-LUNG-O measurements were taken 3–5 m from the temple; the $PM_{2.5}$ exposure levels inside the temple would be much higher than those measurements. Long-term community monitoring can pinpoint those community sources that should be the targets of control strategies.

The AS-LUNG-O set at C-6 is the one without recalibration over the 3.5 years. TMOE station is 800 m away from C-6. The correlation of their measurements is 0.86, ranked 4th among these ten locations (Table 2). Moreover, the R^2 values and slopes of the regression with the TMOE observations (Table S2) and the $PM_{2.5}$ winter maximums from 2017 to 2020 did not show signs of a decreasing trend. Furthermore, based on the individual-location models, C-6 is still identified as the one with the highest contribution of religious activity. This shows that even without calibration, the AS-LUNG-O set still provides a good indication of the $PM_{2.5}$ levels in the community and demonstrates its ability to quantify the contribution of the surrounding sources. These results demonstrate the stability of the sensors used. The regular cleaning at intervals of 1 or 2 months also helps in maintaining the data quality. The fact that this sensor is not re-calibrated may increase the variability of the measurements; nevertheless, the advantage of the sample size outweighs the disadvantage, especially in the statistical analysis. This has important implications for resource-limited research groups which may not have the manpower and resources to conduct annual or even biennial calibration for a LCS network.

There are some limitations of this study. With long-term monitoring, the activities of all sources cannot be recorded in as much detail as they can for intensive monitoring over periods of several days or months. At the start of the monitoring period, our team spent over a month in the community during both summer and winter (Lung et al., 2020a). During these periods, we conducted daily observations, walking through the community more than three times per day to document activities in the surroundings. Our observations revealed that most activities followed routine patterns, except accidental events. Beyond these two intensive monitoring periods, we revisited the monitoring locations every 1 to 2 months. The active periods for all sources included in the regression analysis were determined based on these records. We have confidence that the activity times we used in the model were mostly correct. However, we cannot take into account the accidents, which are out of the scope of the current study. This may have increased the variability of the coefficient estimations, but it does not affect the validity of our results. Additionally, the inherent higher variability in the data obtained from LCSs was a concern; this may result in higher standard errors in the estimates of the regression analysis. Nevertheless, the advantage of a large sample size offsets this impact.

Conclusions

In this study, a network of the calibrated LCSs (AS-LUNG-O) was deployed along community streets for long-term monitoring, capturing $PM_{2.5}$ observations with a sample size sufficient to evaluate long-term trends, hotspots, and $PM_{2.5}$ variations across different classifications. The extended monitoring approach enabled the detection of high $PM_{2.5}$ levels from unexpected or irregular events—insights unattainable through short-term campaigns. We comprehensively evaluated temporospatial $PM_{2.5}$ variations within the community and quantified primary sources of $PM_{2.5}$ exposure at the street level. Our findings reveal that both meteorological factors and religious events statistically significantly influenced $PM_{2.5}$ concentrations. The COVID-19 lockdown period demonstrated a notable decrease in $PM_{2.5}$ concentrations.

The study underscores the potential of research-grade LCS networks in community monitoring. Their cost-effectiveness, operational simplicity, and fine temporospatial resolution empower governmental agencies and citizen groups to assess community $PM_{2.5}$ levels and identify emission sources. This forward-looking approach of integrating advanced sensor technologies into community-scale air quality monitoring can provide the authorities with the evidence for community source controls. Moreover, long-term street-level observations provide representative exposure levels crucial for environmental epidemiological studies assessing the long-term health impacts of $PM_{2.5}$. The methodology demonstrated here offers a transferable framework for $PM_{2.5}$ studies in other countries to facilitate community $PM_{2.5}$ monitoring for the benefit of public health.

Acknowledgements We acknowledge the funding support from Academia Sinica, Taiwan, under the project numbers AS-SS-107-03, AS-SS-110-02, and AS-GC-110-01 and the Taiwan National Science and Technology Council under the project numbers MOST-106-2111-M-001-010, MOST-107-2111-M-001-009, MOST-108-2111-M-001-014, MOST-109-2111-M-001-007, MOST-110-2111-M-001-003, NSTC-112-2123-M-001-008, and NSTC-113-2123-M-001-013. We would also like to thank the research assistants, postdoctoral researchers, and community leaders who assisted in this study.

Author contribution Tzu-Chi Chieh: Formal analysis, Data Curation, Visualization, Writing—Original Draft, Writing—Review & Editing; Shih-Chun Candice Lung: Conceptualization, Methodology, Resources, Writing—Original Draft, Writing—Review & Editing, Supervision, Funding acquisition; Li-Te Chang: Methodology, Investigation, Writing—Review & Editing; Chun-Hu Liu: Investigation, Data Curation, Writing—Review & Editing; Ming-Chien Mark Tsou: Methodology, Investigation, Project administration, Writing—Review & Editing; Tzu-Yao Julia Wen: Investigation, Project administration, Writing—Review & Editing.

Funding Open access funding provided by Academia Sinica. This work was supported by Academia Sinica, Taiwan, under project numbers AS-SS-107–03, AS-SS-110–02, and AS-GC-110–01, and the Taiwan National Science and Technology Council under project numbers MOST-106–2111-M-001–010, MOST-107–2111-M-001–009, MOST-108–2111-M-001–014, MOST-109–2111-M-001–007, MOST-110–2111-M-001–003, NSTC-112–2123-M-001–008, and NSTC-113–2123-M-001–013.

Data availability No datasets were generated or analysed during the current study.

Declarations

Competing interests The authors declare no competing interests.

References

Alexeeff, S. E., Liao, N. S., Liu, X., Van Den Eeden, S. K., Sidney, S. (2021). Long-term $PM_{2.5}$ exposure and risks of ischemic heart disease and stroke events: Review and meta‑analysis. *Journal of the American Heart Association, 10*(1). https://doi.org/10.1161/JAHA.120.016890

Bai, L., Huang, L., Wang, Z., Ying, Q., Zheng, J., Shi, X., & Hu, J. (2020). Long-term field evaluation of low-cost particulate matter sensors in Nanjing. *Aerosol and Air Quality Research, 20*(2), 242–253. https://doi.org/10.4209/aaqr.2018.11.0424

Brunekreef, B., & Holgate, S. T. (2002). Air pollution and health. *The Lancet, 360*(9341), 1233–1242. https://doi.org/10.1016/S0140-6736(02)11274-8

Bulot, F. M., Johnston, S. J., Basford, P. J., Easton, N. H., Apetroaie-Cristea, M., Foster, G. L., … Loxham, M. (2019). Long-term field comparison of multiple low-cost particulate matter sensors in an outdoor urban environment. *Scientific Reports, 9*(1), 7497. https://doi.org/10.1038/s41598-019-43716-3

Chaudhry, S. K., Tripathi, S. N., Reddy, T. V. R., Kumar, A., Madhwal, S., Yadav, A. K., & Pradhan, P. K. (2024). Influence of seasonal variation on spatial distribution of $PM_{2.5}$ concentration using low-cost sensors. *Environmental Monitoring and Assessment, 196*(12), 1234.

Chen, S.-P., Chang, C.-C., Liu, J.-J., Chou, C.C.-K., Chang, J. S., & Wang, J.-L. (2014). Recent improvement in air quality as evidenced by the island-wide monitoring network in Taiwan. *Atmospheric Environment, 96*, 70–77. https://doi.org/10.1016/j.atmosenv.2014.06.060

Chou, C. C.-K., Lung, S.-C. C., Hsiao, T.-C., spsampsps Lee, C.-T. (2023). Regional and urban air quality in East Asia: Taiwan. In: *Handbook of Air Quality and Climate Change* (pp. 1–38).

Chu, H.-J., Ali, M. Z., He, Y.-C. (2020). Spatial calibration and $PM_{2.5}$ mapping of low-cost air quality sensors. *Scientific Reports, 10*(1), 22079. https://doi.org/10.1038/s41598-020-79064-w

Connolly, R. E., Yu, Q., Wang, Z., Chen, Y. H., Liu, J. Z., Collier-Oxandale, A., ... Zhu, Y. (2022). Long-term evaluation of a low-cost air sensor network for monitoring indoor and outdoor air quality at the community scale. *Science of The Total Environment, 807*, 150797. https://doi.org/10.1016/j.scitotenv.2021.150797

Fang, G.-C., Chang, C.-N., Chu, C.-C., Wu, Y.-S., Pi-Cheng Fu, P., Chang, S.-C., Yang, I. L. (2003). Fine ($PM_{2.5}$), coarse ($PM_{2.5–10}$), and metallic elements of suspended particulates for incense burning at Tzu Yun Yen temple in central Taiwan. *Chemosphere, 51*(9), 983–991. https://doi.org/10.1016/S0045-6535(03)00124-3

Farooqui, Z., Biswas, J., & Saha, J. (2023). Long-term assessment of purpleair low-cost sensor for $PM_{2.5}$ in California, USA. *Pollutants, 3*(4), 477–493. https://doi.org/10.3390/pollutants3040033

Feenstra, B., Papapostolou, V., Hasheminassab, S., Zhang, H., Der Boghossian, B., Cocker, D., & Polidori, A. (2019). Performance evaluation of twelve low-cost $PM_{2.5}$ sensors at an ambient air monitoring site. *Atmospheric Environment, 216*, 116946. https://doi.org/10.1016/j.atmosenv.2019.116946

Feng, Z., Zheng, L., Ren, B., Liu, D., Huang, J., & Xue, N. (2024). Feasibility of low-cost particulate matter sensors for long-term environmental monitoring: Field evaluation and calibration. *Science of the Total Environment, 945*, Article 174089.

Franklin, M., Vora, H., Avol, E., McConnell, R., Lurmann, F., Liu, F., … Gauderman, W. J. (2012). Predictors of intra-community variation in air quality. *Journal of Exposure Science & Environmental Epidemiology, 22*(2), 135–147. https://doi.org/10.1038/jes.2011.45

Gao, M., Cao, J., & Seto, E. (2015). A distributed network of low-cost continuous reading sensors to measure spatiotemporal variations of $PM_{2.5}$ in Xi'an, China*Environmental Pollution, 199*, 56–65. https://doi.org/10.1016/j.envpol.2015.01.013

Gualtieri, G., Brilli, L., Carotenuto, F., Cavaliere, A., Giordano, T., Putzolu, S., ... Gioli, B. (2024). Performance assessment of two low-cost $PM_{2.5}$ and PM_{10} monitoring networks in the Padana Plain (Italy). *Sensors, 24*(12), 3946. https://doi.org/10.3390/s24123946

Heintzelman, A., Filippelli, G. M., Moreno-Madriñan, M. J., Wilson, J. S., Wang, L., Druschel, G. K., & Lulla, V. O. (2023). Efficacy of low-cost sensor networks at detecting fine-scale variations in particulate matter in urban environments. *International Journal of Environmental Research and Public Health, 20*(3), 1934. https://doi.org/10.3390/ijerph20031934

Hou, K., & Xu, X. (2021). Evaluation of the influence between local meteorology and air quality in Beijing using generalized additive models. *Atmosphere, 13*(1), 24. https://doi.org/10.3390/atmos13010024

Hsu, W.-T., Chen, J.-L., Candice Lung, S.-C., & Chen, Y.-C. (2020). $PM_{2.5}$ exposure of various microenvironments in a community: Characteristics and applications. *Environmental Pollution, 263*, 114522. https://doi.org/10.1016/j.envpol.2020.114522

Jayaratne, R., Liu, X., Ahn, K. H., Asumadu-Sakyi, A., Fisher, G., Gao, J., … Nyaku, M. (2020). Low-cost $PM_{2.5}$ sensors: An assessment of their suitability for various applications. *Aerosol and Air Quality Research, 20*(3), 520–532. https://doi.org/10.4209/aaqr.2018.10.0390

Jiao, W., Hagler, G., Williams, R., Sharpe, R., Brown, R., Garver, D., … Davis, M. (2016). Community Air Sensor Network (CAIRSENSE) project: Evaluation of low-cost sensor performance in a suburban environment in the southeastern United States. *Atmospheric Measurement Techniques, 9*(11), 5281-5292. https://doi.org/10.5194/amt-9-5281-2016

Johnson, K. K., Bergin, M. H., Russell, A. G., & Hagler, G. S. (2018). Field test of several low-cost particulate matter sensors in high and low concentration urban environments. *Aerosol and Air Quality Research, 18*(3), 565. https://doi.org/10.4209/aaqr.2017.10.0418

Karagulian, F., Belis, C. A., Dora, C. F. C., Prüss-Ustün, A. M., Bonjour, S., Adair-Rohani, H., & Amann, M. (2015). Contributions to cities' ambient particulate matter (PM): A systematic review of local source contributions at global level. *Atmospheric Environment, 120*, 475–483. https://doi.org/10.1016/j.atmosenv.2015.08.087

Kelly, K., Whitaker, J., Petty, A., Widmer, C., Dybwad, A., Sleeth, D., … Butterfield, A. (2017). Ambient and laboratory evaluation of a low-cost particulate matter sensor. *Environmental Pollution, 221*, 491–500. https://doi.org/10.1016/j.envpol.2016.12.039

Kim, S., Go, H., Bang, E., & Jung, K. (2025). Field performance evaluation of low-cost $PM_{2.5}$ sensors for enhancing spatial resolution of $PM_{2.5}$ monitoring: A case study in the smart city of Sejong, Korea. *Environmental Monitoring and Assessment, 197*(1), 1–13.

Kioumourtzoglou, M.-A., Schwartz, J. D., Weisskopf, M. G., Melly, S. J., Wang, Y., Dominici, F., & Zanobetti, A. (2016). Long-term $PM_{2.5}$ exposure and neurological hospital admissions in the northeastern United States. *Environmental Health Perspectives, 124*(1), 23–29. https://doi.org/10.1289/ehp.1408973

Kosmopoulos, G., Salamalikis, V., Matrali, A., Pandis, S. N., & Kazantzidis, A. (2022). Insights about the sources of $PM_{2.5}$ in an urban area from measurements of a low-cost sensor network. *Atmosphere, 13*(3), 440. https://doi.org/10.3390/atmos13030440

Kurniawati, S., Santoso, M., Nurhaini, F. F., Atmodjo, D. P. D., Lestiani, D. D., Ramadhani, M. F., ... Tursinah, R. (2025). Assessing low-cost sensor for characterizing temporal variation of $PM_{2.5}$ in Bandung, Indonesia. *Kuwait Journal of Science, 52*(1), 100297. https://doi.org/10.1016/j.kjs.2024.100297

Latif, M. T., Purhanudin, N., Afandi, N. Z. M., Cambaliza, M. O. L., Halim, N. D. A., Hawari, N. S. S. L., Hien, T. T., Hlaing, O. M. T., Jansz, W. R. L. H., Khokhar, M. F., Lestari, P., Lung, S.-C. C., Naja, M., Oanh, N. T. K., Othman, M., Salam, A., Salim, P. M., Song, C.-K., Fujinawa, T., … Crawford, J. H. (2024). In-depth analysis of ambient air pollution changes due to the COVID-19 pandemic in the Asian Monsoon region. *Science of the Total Environment*. https://doi.org/10.1016/j.scitotenv.2024.173145

Lee, C.-H., Lung, S.-C. C., & Chen, J.-P. (2023). Three-dimensional spatial inhomogeneity of traffic-generated urban $PM_{2.5}$ in street canyons. *Atmospheric Pollution Research, 14*(5), 101748. https://doi.org/10.1016/j.apr.2023.101748

Lee, Y.-M., Lin, G.-Y., Le, T.-C., Hong, G.-H., Aggarwal, S. G., Yu, J.-Y., & Tsai, C.-J. (2024). Characterization of spatial-temporal distribution and microenvironment source contribution of $PM_{2.5}$ concentrations using a low-cost sensor network with artificial neural network/kriging techniques. *Environmental Research, 244*, 117906. https://doi.org/10.1016/j.envres.2023.117906

Lewis, A., Peltier, W. R., & von Schneidemesser, E. (2018). Low-cost sensors for the measurement of atmospheric composition: Overview of topic and future applications. *Research Report*. World Meteorological Organization (WMO).

Li, Z., Ho, K.-F., Chuang, H.-C., & Yim, S. H. L. (2021). Development and intercity transferability of land-use regression models for predicting ambient PM_{10}, $PM_{2.5}$, NO_2 and O_3 concentrations in northern Taiwan. *Atmospheric Chemistry and Physics, 21*(6), 5063-5078. https://doi.org/10.5194/acp-21-5063-2021

Liu, X., Jayaratne, R., Thai, P., Kuhn, T., Zing, I., Christensen, B., … Morawska, L. (2020). Low-cost sensors as an alternative for long-term air quality monitoring. *Environmental Research, 185*, 109438. https://doi.org/10.1016/j.envres.2020.109438

Lung, S.-C. C., Wang, W.-C. V., Wen, T.-Y. J., Liu, C.-H., & Hu, S.-C. (2020a). A versatile low-cost sensing device for assessing $PM_{2.5}$ spatiotemporal variation and quantifying source contribution. *Science of The Total Environment, 716*, 137145. https://doi.org/10.1016/j.scitotenv.2020.137145

Lung, S. C. C., Chen, N., Hwang, J. S., Hu, S. C., Wang, W. C. V., Wen, T. Y. J., & Liu, C. H. (2020b). Panel study using novel sensing devices to assess associations of PM(2.5) with heart rate variability and exposure sources. *Journal of Exposure Science and Environmental Epidemiology*, *30*(6), 937–948. https://doi.org/10.1038/s41370-020-0254-y

Lung, S.-C.C., Hsiao, P.-K., Wen, T.-Y., Liu, C.-H., Fu, C. B., & Cheng, Y.-T. (2014). Variability of intra-urban exposure to particulate matter and CO from Asian-type community pollution sources. *Atmospheric Environment, 83*, 6–13. https://doi.org/10.1016/j.atmosenv.2013.10.046

Lung, S.-C.C., Mao, I.-F., & Liu, L.-J.S. (2007). Residents' particle exposures in six different communities in Taiwan. *Science of the Total Environment, 377*(1), 81–92. https://doi.org/10.1016/j.scitotenv.2007.01.092

Ministry of Health and Welfare. (2021). *Timeline COVID-19 in Taiwan*, Taiwan government. Accessed 18 June 2024. https://covid19.mohw.gov.tw/en/sp-timeline0-206.html

Ouimette, J., Arnott, W. P., Laven, P., Whitwell, R., Radhakrishnan, N., Dhaniyala, S., Sandink, M., Tryner, J., & Volckens, J. (2024). Fundamentals of low-cost aerosol sensor design and operation. *Aerosol Science and Technology, 58*(1), 1–15. https://doi.org/10.1080/02786826.2023.2285935

Rojas González, L., & Montilla-Rosero, E. (2025). Evaluation of in-situ low-cost sensor network in a Tropical Valley, Colombia*Sensors, 25*(4), 1236. https://doi.org/10.3390/s25041236

Rose Eilenberg, S., Subramanian, R., Malings, C., Hauryliuk, A., Presto, A. A., & Robinson, A. L. (2020). Using a network of lower-cost monitors to identify the influence of modifiable factors driving spatial patterns in fine particulate matter concentrations in an urban environment. *Journal of Exposure Science & Environmental Epidemiology, 30*(6), 949–961. https://doi.org/10.1038/s41370-020-0255-x

Sinnreich, R., Kark, J. D., Friedlander, Y., Sapoznikov, D., & Luria, M. H. (1998). Five minute recordings of heart rate variability for population studies: Repeatability and age-sex characteristics. *Heart, 80*(2), 156–162. https://doi.org/10.1136/hrt.80.2.156

Song, Y.-Z., Yang, H.-L., Peng, J.-H., Song, Y.-R., Sun, Q., & Li, Y. (2015). Estimating $PM_{2.5}$ concentrations in Xi'an city using a generalized additive model with multi-source monitoring data. *PLoS One, 10*(11), e0142149. https://doi.org/10.1371/journal.pone.0142149

Tseng, C.-H., Chen, L. L., & Tseng, G.-H. (2021). Applying low-cost air-pollution sensors' information to explore $PM_{2.5}$ concentration with an emphasis on spatial and temporal analysis: A case in Chiayi city. *Research Square*. https://doi.org/10.21203/rs.3.rs-796520/v1

Tsou, M.-C. M., Lung, S.-C. C., & Cheng, C.-H. (2021a). Demonstrating the applicability of smartwatches in $PM_{2.5}$ health impact assessment. *Sensors, 21*(13), 4585. https://doi.org/10.3390/s21134585

Tsou, M.-C. M., Lung, S.-C. C., Shen, Y.-S., Liu, C.-H., Hsieh, Y.-H., Chen, N., & Hwang, J.-S. (2021b). A community-based study on associations between $PM_{2.5}$ and PM_1 exposure and heart rate variability using wearable low-cost sensing devices. *Environmental Pollution, 277*, 116761. https://doi.org/10.1016/j.envpol.2021.116761

Wang, W.-C. V., Lung, S.-C. C., & Liu, C.-H. (2020a). Application of machine learning for the in-field correction of a $PM_{2.5}$ low-cost sensor network. *Sensors, 20*(17), 5002. https://doi.org/10.3390/s20175002

Wang, W.-C.V., Lung, S.-C.C., Liu, C. H., & Shui, C.-K. (2020b). Laboratory evaluations of correction equations with multiple choices for seed low-cost particle sensing devices in sensor networks. *Sensors, 20*(13), 3661. https://doi.org/10.3390/s20133661

WHO. (2021). WHO global air quality guidelines: Particulate matter ($PM_{2.5}$ and PM_{10}), ozone, nitrogen dioxide, sulfur dioxide and carbon monoxide. World Health Organization.

WHO. (2023). *WHO ambient air quality database, 2022 update: Status report*. World Health Organization.

Wolf, K., Cyrys, J., Harciníková, T., Gu, J., Kusch, T., Hampel, R., Schneider, A., & Peters, A. (2017). Land use regression modeling of ultrafine particles, ozone, nitrogen oxides and markers of particulate matter pollution in Augsburg. *Science of the Total Environment, 579*, 1531–1540. https://doi.org/10.1016/j.scitotenv.2016.11.160

Wong, Y. J., Shiu, H. Y., Chang, J. H. H., Ooi, M. C. G., Li, H. H., Homma, R., Shimizu, Y., Pei-Te, C., Maneechot, L., & Sulaiman, N. M. N. (2022). Spatiotemporal impact of COVID-19 on Taiwan air quality in the absence of a lockdown: Influence of urban public transportation use and meteorological conditions. *Journal of Cleaner Production, 365*, Article 132893. https://doi.org/10.1016/j.jclepro.2022.132893.

Wu, C.-D., Chen, Y.-C., Pan, W.-C., Zeng, Y.-T., Chen, M.-J., Guo, Y. L., & Lung, S.-C.C. (2017). Land-use regression with long-term satellite-based greenness index and culture-specific sources to model $PM_{2.5}$ spatial-temporal variability. *Environmental Pollution, 224*, 148–157. https://doi.org/10.1016/j.envpol.2017.01.074

Xu, M., Sbihi, H., Pan, X., & Brauer, M. (2019). Local variation of $PM_{2.5}$ and NO_2 concentrations within metropolitan Beijing. *Atmospheric Environment, 200*, 254–263.

Zheng, T., Bergin, M. H., Johnson, K. K., Tripathi, S. N., Shirodkar, S., Landis, M. S., … Carlson, D. E. (2018). Field evaluation of low-cost particulate matter sensors in high- and low-concentration environments. *Atmospheric Measurement Techniques, 11*(8), 4823-4846. https://doi.org/10.5194/amt-11-4823-2018

Zwack, L. M., Paciorek, C. J., Spengler, J. D., & Levy, J. I. (2011). Modeling spatial patterns of traffic-related air pollutants in complex urban terrain. *Environmental Health Perspectives, 119*(6), 852–859. https://doi.org/10.1289/ehp.1002519